

TABLES

Table S1: Time- and cost-savings estimates for j5 compared with traditional cloning and DNA synthesis

| Task | | Traditional cloning ¹ and robotics ⁴ | DNA Synthesis ² | SLIC/Gibson/CPEC ³ with j5 and robotics ⁴ | Golden Gate with j5 and robotics ⁴ |
|------|----------------------------|--|--|---|---|
| A | Hands-on time ⁵ | 5.7 hr design 6.7 hr lab | 0.1 hr design ⁶ 0.1 hr order | 1.2 hr design 4.4 hr lab | 0.4 hr design 4.4 hr lab |
| | Materials cost | \$212 | \$2345 | \$174 | \$174 |
| | Total cost | \$1452 | \$2365 | \$734 | \$654 |
| | Total duration | 2.5 weeks | 2 months | 2 weeks | 2 weeks |
| B | Hands-on time | 3.1 hr design 4.1 hr lab | 0.1 hr design 0.1 hr order | 0.5 hr design 4.2 hr lab | 0.2 hr design 4.2 hr lab |
| | Materials cost | \$73 | \$785 | \$64 | \$64 |
| | Total cost | \$793 | \$805 | \$534 | \$504 |
| | Total duration | 2 weeks | 3 weeks | 2 weeks | 2 weeks |
| C | Hands-on time | 176.3 hr design 767.0 hr lab | 20.3 hr design 20.3 hr order | N/A | 29.0 hr design ⁷ 82.9 hr lab ⁸ |
| | Materials cost | \$27,813 ⁹ | \$533,535 | | \$18,686 ⁹ |
| | Total cost | \$122,143 | \$537,585 | | \$29,876 |
| | Total duration | 11 months | 2.3 months | | 1.5 months |
| D | Hands-on time | 67.9 hr design 229.9 hr lab | 18.0 hr design 18.0 hr order | N/A | 7.8 hr design ⁷ 74.9 hr lab ⁸ |
| | Materials cost | \$8,102 ⁹ | \$137,310 | | \$5,834 ⁹ |
| | Total cost | \$37,882 | \$140,910 | | \$14,104 |
| | Total duration | 3.5 months | 1 month | | 1.3 months |

DNA construction tasks:

- A) Metabolic pathway construction: vector backbone 4kb + 2 promoters (200 bp each) + 5 ORFs (with RBS, 1000 bp each) + 1 terminator (100 bp)
- B) Protein chimera construction: vector backbone 4kb + 3 domains (500 bp each)
- C) Combinatorial library (243 constructs = 3⁵ [3 orthologs for each of the 5 ORFs]) of task A) above
- D) Combinatorial library (216 constructs = 6³ [6 orthologs for each of the 3 domains]) of task B) above

¹Best-case scenario (viable restriction enzyme choices). Binary ligations with maximum intermediate re-use.

²Assumes perfect parallel process scaling, \$0.39/bp, \$50/construct for custom destination vector.

³SLIC/Gibson/CPEC can be used interchangeably to assemble the same j5-designed fragments (see Results).

⁴No automation of transformation/clonal isolation process

⁵Fully burdened-labor cost estimate: \$100/hr. Design time includes sequence validation.

⁶Design time refers here to DNA sequence file manipulation (i.e., pasting each insert into the vector backbone)

⁷Almost exclusively sequence validation

⁸Almost exclusively transformation/clonal isolation processes

⁹Dominated by DNA sequencing service costs (\$2.50 per 800-bp read)

METHODS

All DNA sequences and *E. coli* strains identified as JPUB_XXXXXX have been accessioned in the JBEI public registry (<http://public-registry.jbei.org>) and are available upon request. j5 design files, related oligo lists, and chromatogram sequence trace files are linked to the JPUB entries and can be downloaded or viewed there.

Plasmid pNJH00010 construction

Plasmid pNJH00010 (JPUB_000226) was constructed as designed by j5 (see the j5 design file pNJH00010.csv that is attached to the pNJH00010 registry entry). Briefly, plasmid pBbs8c-RFP (1) (JPUB_000041) was purified from *E. coli* strain JBEI-2566 (JPUB_000199) by Qiagen miniprep kit (per manufacturer's instructions), 3.5 μ g was digested with 25 units each *EcoRI* and *XhoI* (Fermentas), and the vector backbone fragment gel purified (Qiagen). Insert parts were generated by PCR using Phusion polymerase (New England Biosciences, manufacturer's instructions) and primers RDR00130/132, RDR00134/136, and RDR00138/140 (see the pNJH00010.csv design file for the primer specifications). For the initial SLIC chew-back step, 360 ng of each assembly piece was digested with T4 DNA polymerase. Subsequently, 275 ng digested backbone was combined with equimolar parts 1 & 3, and 4-fold molar excess of part 2 due to its small size to mitigate the risk of excessive exonuclease degradation. The CPEC and Gibson assembly reactions used 100 ng vector, equimolar parts 1 and 3, and 4-fold molar excess part 2. Assembly reactions proceeded according to published methods (2-4) and 5 μ L each reaction was transformed into 100 μ L Keasling-1484 (*E. coli* DH10b Δ *araFGH* Δ *araE* $P_{CP18}::araE$ (1)) chemically competent cells, yielding strain JBEI-2804 (JPUB_000235). Transformants were selected for on LB-agar plates with 30 μ g/mL chloramphenicol, and screened by PCR (primers RDR00001 and RDR00142, see the DNA_oligo_file.csv attached to the pNJH00010 registry entry for the primer specifications) for the correct inserts. Plasmid DNA was isolated by miniprep (Qiagen kit) and the success of plasmid assembly verified by Sanger sequencing of plasmid DNA (sequencing trace files are attached to the Seq. Analysis tab of the pNJH00010 registry entry).

Construction of plasmids pRDR00001 – pRDR00008

Eight GFPuv-signal peptide plasmid variants (pRDR00001 – pRDR00008; JPUB_000227-234) were assembled by the Golden Gate method (5, 6) from linear PCR products amplified from pNJH00010. Specifications of all oligos, PCR reactions, and assembly combinations are provided in the j5 design files attached to the respective JBEI public registry entries. Briefly, the vector backbone was amplified with primers incorporating either a *sig1* or *sig2* signal peptide, and the *gfpuv* open reading frame was amplified with primers incorporating either a long or short linker sequence at the 5' end of the gene and either a regular or enhanced *ssrA* tag at the 3' end of the gene. PCR amplicons were purified by Qiagen column (manufacturer's instructions) and DNA concentrations determined by nanodrop. Golden Gate assembly reactions were set up in 15 μ L containing 100 ng vector backbone and equimolar insert, 1/10th volume 10X T4 DNA ligase buffer, 2,000 cohesive end units T4 DNA ligase (i.e. 1 μ L high concentration) and 10 units *BsaI* (all enzymes, New England Biosciences). Reactions proceeded at 37°C for 1 hour, followed by 5 minute incubations at 50°C and 80°C. Five μ L of each reaction was transformed into *E. coli* strain Keasling-1484 (1), yielding strains JBEI-2747-9,2923,2751-3,2755 (JPUB_000236-43) and cells plated on LB-agar with 30 μ g/mL chloramphenicol. Transformants were screened by colony PCR, plasmid DNA isolated by miniprep (Qiagen kit) and the success of plasmid assembly verified by Sanger sequencing of plasmid DNA (sequencing trace files are attached to the Seq. Analysis tab of the pRDR00001 – pRDR00008 registry entries).

Markerless deletion of *clpX*

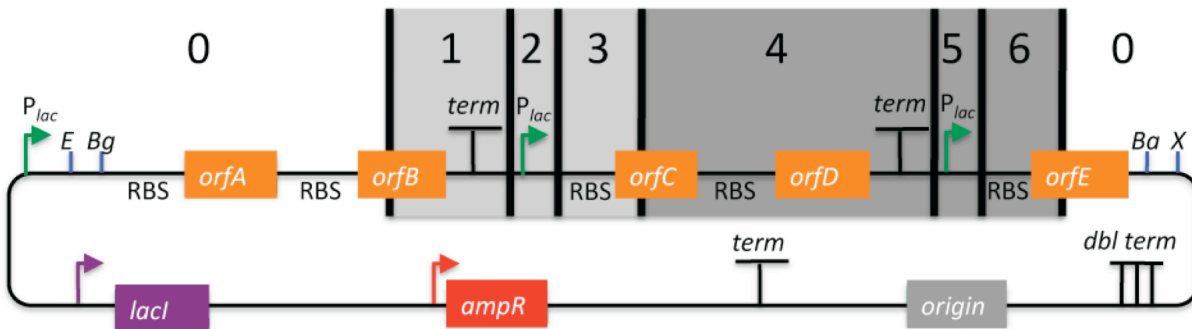
In order to test the efficacy of the *ssrA* degradation tag on the GFPuv variants, the protease encoding gene *clpX* was removed from the Keasling-1484 (1) genome by a markerless deletion strategy (7) (see also Figure S8). Keasling-1484 was transformed with pREDI (7) (JPUB_000019), encoding the lambda red recombinase machinery under the control of P_{bad} and *I-SceI* homing endonuclease under the control of P_{rhaB} with a temperature sensitive origin of replication, resulting in strain JBEI-2948 (JPUB_000253). A j5-designed linear deletion cassette containing a kanamycin resistance marker, *sacB* sucrose counter-selection marker, *I-SceI* cleavage motif, and genomic sequence flanking *clpX* for targeted recombination regions was amplified using Phusion polymerase and primers RDR00044 and RDR00045 from template pSKI (7) (JPUB_000270), resulting in DNA part Δ *clpX*_cassette (JPUB_000255) (see the j5 design file D*clpX*_j5_design.csv that is attached to the Δ *clpX*_cassette registry entry). Because our aim was to generate a linear cassette rather than a circularized plasmid, these primers were manually modified from the j5 design file to remove the 5' overlapping regions

introduced by the software. Due to the length of the oligos and formation of inhibitory primer dimers, successful amplification required the addition of 1M betaine, 5% DMSO, and 50 μ M 7deaza-GTP (8). Amplicons were incubated with 10 units *DpnI* for 1 hour at 37°C, gel purified, and concentrated to ~ 100 ng/ μ L. Four μ L (400 ng) of deletion cassette was transformed into electrocompetent JBEI-2948, cells were recovered at 30°C, and plated on LB-agar with 100 μ g/mL ampicillin, 50 μ g/mL kanamycin, and 10 mM arabinose. Four recovered clones were screened by colony PCR with primers flanking (RDR00050/051) and specific to (RDR00050/052) the inserted deletion cassette (see the DNA_oligo_file.csv attached to the Δ clpX_cassette registry entry for the primer specifications). Those colonies yielding the expected PCR products were replica plated on LB-agar with ampicillin and kanamycin versus LB-agar with ampicillin and sucrose. One of the two clones demonstrating kanamycin resistance and sucrose sensitivity was archived as JBEI-3080 (JPUB_000269). The insertion cassette was then excised by growing JBEI-3080 to O.D.₆₀₀ ~ 0.4 in LB plus ampicillin and 10 mM rhamnose over three 10% dilutions and plating on LB-agar plus ampicillin, rhamnose and 5% sucrose. Recovered colonies were replica plated on agar containing either sucrose or kanamycin, and strain JBEI-3083 (JPUB_000254) was selected for sucrose growth and kanamycin sensitivity. Markerless deletion was confirmed by colony PCR using flanking and insert specific primers, as above, and by Sanger sequencing of the resulting amplicons (sequencing trace files are attached to the Seq. Analysis tab of the JBEI-3083 registry entry).

GFP expression from plasmid variants

Plasmid pNJH00010 and each GFPuv plasmid variant were transformed by heat shock into chemically competent JBEI-3083, resulting in strains JBEI-3144,3133-40 (JPUB_000244-52). Recovered colonies were grown overnight at 42°C to cure pREDI and restreaked on LB-agar plus chloramphenicol. Cells harboring the GFPuv plasmid but not pREDI were selected by colony PCR. Four colonies per plasmid variant for each host JBEI-3083 and Keasling-1484 (1) were grown overnight in deep well 96-well plates containing 1 mL LB + 30 μ g/mL chloramphenicol per well. These were diluted 1:100, grown to an average O.D. ~ 0.2, induced with 5 mM arabinose, and grown an additional 6 hours. Cells were pelleted, washed twice in M9 minimal media, and GFP fluorescence and optical density measured in duplicate in a SpectroMax Plus384 (Molecular Devices) plate reader.

order list example. The user must specify the sequential order (from top to bottom, first column) of the parts to be assembled together, the direction of each part (second column), and as well as optionally whether to force j5 to use a particular assembly strategy for each part (third column), whether to force j5 to use a particular relative overhang position (in bp, Golden Gate assembly only) following each part (fourth column), and whether to place a direct DNA synthesis firewall following each part (fifth column). **(D)** Combinatorial library target part order list example. The user must specify the sequential order (from top to bottom, first column) of the combinatorial part bins to be assembled together (each denoted by a leading '>' character, grey rows) and the parts within each bin (immediately following each bin name). Other columns are as in (C). **(E)** Eugene design specification rules example file. When designing assemblies with j5, it is possible to set design specification rules that limit the total number of times a given part appears in a given assembly (**NOTMORETHAN** statements, rules r1-r9), if two given parts should not appear together in the same assembly (**NOTWITH** statements, rules r10-r11), or if two given parts should only appear together in the same assembly (**WITH** statement, rules r12-r15). The design specification rules understood by j5 (shown as those shown here) are derived from (and are a strict subset of) the Eugene biological design specification computer language (9, 10). **(F)** Example j5 parameters CSV input file, stylized for clarity. The user may optionally change parameter values by modifying entries in the second column. Default values (third column) and descriptions (fourth column) are provided as a reference for each parameter. **(G)** Example Target Part Ordering/Selection/Strategy section of an assembly design CSV output file, stylized for clarity. The assembly order (top to bottom) and direction (fourth column), and the optimal assembly strategy (as determined by Algorithm S1, fifth column), are shown for each part to be assembled (third column).

A**B**

| Incompatibilities between Assembly Pieces: | | |
|--|----------|-----------|
| Assembly Piece | Left End | Right End |
| 0 | NONE | NONE |
| 1 | NONE | 0, 4, 5 |
| 2 | NONE | 5, 6 |
| 3 | 0, 5, 6 | NONE |
| 4 | NONE | 0, 2 |
| 5 | NONE | 2, 3 |
| 6 | 0, 2, 3 | NONE |

C

| Suggested Assembly Piece Contigs For Hierarchical Assembly: | |
|---|---------------------------|
| Contig | Assembly Pieces Contained |
| 0 | 0 |
| 1 | 1, 2, 3 |
| 2 | 4, 5, 6 |

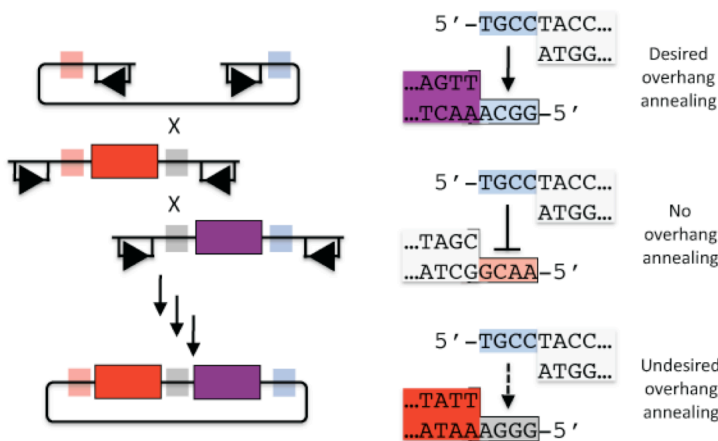
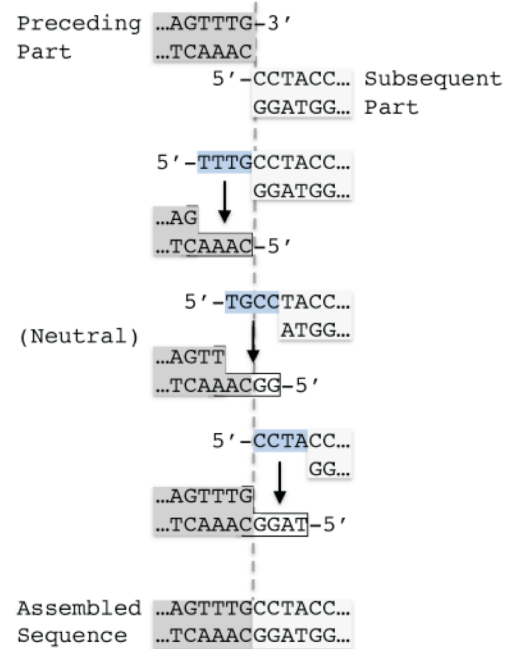
D**E**

Figure S2. The search for compatible sets of homology and overhang sequences. **(A-C)** SLIC, Gibson, and CPEC assembly piece putative incompatibilities. **(A)** Schematic of a hypothetical plasmid to be assembled, demarcated at the boundaries of DNA assembly pieces “0” through “6”. Pieces “2” and “5” are identical, containing the P_{lac} promoter, which is also internally present in piece “0”. **(B)** j5-predicted assembly piece incompatibilities. The right end of assembly piece “4” (which contains 3’ flanking sequence homologous to the 5’ end of the P_{lac} in piece “5”) is incompatible with assembly pieces “0” and “2”. **(C)** j5 utilizes Algorithm S3 to design a hierarchical assembly strategy that circumvents these incompatibilities by first SOEing together pieces “1”, “2” and “3” (Contig 1), and separately “4”, “5”, “6” (Contig 2), and then assembling together Contig 0 (fragment “0”) with Contig 1 and Contig 2. **(D-E)** Search for optimal Golden Gate overhang sequences. j5 utilizes Algorithm S4 to search through all possible combinations of putative overhang sequences (constrained by the maximum oligo size and the extents of combinatorial sequence identity about each assembly junction) and selects the set of overhangs that 1) are compatible with themselves and each other, and that 2) are as

neutral as possible. **(D)** An example three-part (vector backbone, red part, purple part) Golden Gate assembly with red, grey, and blue overhang junctions. Directional type IIs endonuclease (e.g. *BsaI*) recognition sites are schematically indicated by rectangular boxes below the DNA strand, with arrowheads pointing to the adjacent cut site. Checking for overhang compatibility consists of making sure that (top right) each single stranded overhang sequence (e.g. "TGCC", blue top overhang) is cohesive with its desired cognate partner (e.g. "GGCA", blue bottom overhang), but not with itself nor with off-target sequences (e.g. "AACG", red bottom overhang, middle right). If an overhang is sufficiently cohesive with an off-target sequence (e.g. "GGGA", grey bottom overhang, bottom right, 3 cohesive base-pairs), the set of overhang sequences is declared incompatible and rejected. **(E)** Three possible Golden Gate overhang sequence options (blue sequences) are shown for a particular assembly junction that each result in the scar-less assembly of the preceding part (top left, grey sequence) and the subsequent part (top right, white sequence) into the desired assembled sequence (bottom). The first overhang sequence selection "TTTG" (top) draws all four base pairs from the preceding part (a negative 2-bp relative overhang position), the second selection "TGCC" (middle) draws two base pairs from the preceding part and two from the subsequent part (a neutral overhang), and the third selection "CCTA" (bottom) draws all four base pairs from the subsequent part (a positive 2-bp relative overhang position).

A

| Oligo Name | Length | Tm | Tm (3' only) | Sequence |
|--|--------|--------|--------------|---|
| j5_00001_(gfpuv_sigpep_5prime)_pure_forward | 34 | 60.208 | 60.208 | ATGAGTAAAGGAGAAGCACTTTCTACTGAGTTG |
| j5_00002_(RBS)_gfpuv_sigpep_5prime_forward | 85 | 70.595 | 60.208 | CTGTTTCTCCATACCCGTTTTTGGGAATTTTAAGAGGAGATACATATGAGTAAAGGAGAAGCACTTTCTACTGAGTTG |
| j5_00003_(gfpuv_sigpep_5prime)_pure_reverse | 29 | 60.947 | 60.947 | TCGAGTTTGTGGCGAAGATGTTCCATC |
| j5_00004_(gfpuv_sigpep_5prime)_gfpuv_sigpep_XhoI_silent_reverse | 49 | 67.149 | 60.947 | TCGAGTAAAGGAGAAGCACTTTCTACTGAGTTGTCGAGAAATGTTCCATC |
| j5_00005_(gfpuv_sigpep_middle)_pure_forward | 35 | 60.084 | 60.084 | TACAACATAACTCACACAATGTATACATCACGGC |
| j5_00006_(gfpuv_sigpep_middle)_forward | 57 | 68.942 | 60.084 | CATTCTCGACACAACATCGAATCAACTTAACACACAATGTATACATCACGGC |
| j5_00007_(gfpuv_sigpep_middle)_pure_reverse | 23 | 56.6 | 56.6 | GATCCACTTCAATGTGTGGCG |
| j5_00008_(gfpuv_sigpep_middle)_gfpuv_sigpep_BamHI_silent_reverse | 40 | 68.06 | 56.6 | GGTCTGTAATGTAACAGATCACTTCAATGTGTGGCG |
| j5_00009_(gfpuv_sigpep_3prime)_pure_forward | 36 | 60.484 | 60.484 | GTCCAACTAGGAGACCATATCAACAAAATCTCCA |
| j5_00010_(gfpuv_sigpep_3prime)_forward | 53 | 67.614 | 60.484 | ACATTGAAGATGGATCTTCACTAGCAGACCATATCAACAAAATCTCCA |
| j5_00011_(gfpuv_sigpep_3prime)_pure_reverse | 25 | 60.961 | 60.961 | TTTAGCGATCGGGAACTGCCTCT |
| j5_00012_(gfpuv_sigpep_3prime)_reverse | 57 | 71.658 | 60.961 | GTTTTATTGATCGCTGGAGACTCTTACTGCTTGTAGCGATCGGGAACTGCCTCT |
| j5_00013_(pS8c-gfpuv_sig_pep_vector_backbone)_pure_forward | 34 | 61.437 | 61.437 | AGTAAAGGAGAAGCACTTTCTACTGAGTTGTC |
| j5_00014_(pS8c-gfpuv_sig_pep_vector_backbone)_forward | 49 | 68.643 | 61.437 | TTTTTGGTCTCAGCACTAAAGGAGAAGCACTTTCTACTGAGTTGTC |
| j5_00015_(pS8c-gfpuv_sig_pep_vector_backbone)_pure_reverse | 36 | 57.245 | 57.245 | ATCTATATCTCTCTTAAAATTCACAAAACG |
| j5_00016_(pS8c-gfpuv_sig_pep_vector_backbone)_reverse | 50 | 63.16 | 57.245 | TTTTTGGTCTCATAATGATATATCTCTCTTAAAATTCACAAAACG |
| j5_00017_(umuD_tag)_pure_forward | 34 | 66.451 | 66.451 | ATGTTTGTATCAAGCTCGCGATCTCCGGAAA |
| j5_00018_(umuD_tag)_forward | 50 | 70.629 | 66.451 | TTTTTGGTCTCAGCACTATGTTTATCAAGCTCGCGATCTCCGGAAA |
| j5_00019_(umuD_tag)_pure_reverse | 20 | 61.777 | 61.777 | GCACCCAGATCGCGCT |
| j5_00020_(umuD_tag)_reverse | 35 | 68.828 | 61.777 | TTTTTGGTCTCAGCACTCGCGATCGCGCT |
| j5_00021_(pS8c-vector_backbone)_pure_forward | 28 | 58.876 | 58.876 | TAAATCGAGTAAAGTCTCAGGACATCA |
| j5_00022_(ssrA_tag_3prime)_pS8c-vector_backbone_forward | 59 | 74.575 | 58.876 | TTTTTGGTCTCAAATCGCTGGCGGCTAAATCGAGTAAAGTCTCAGGACATCA |
| j5_00023_(pS8c-vector_backbone)_pure_reverse | 32 | 54.025 | 54.025 | CATATGATATCTCTTAAAATTCACAAA |
| j5_00024_(pS8c-vector_backbone)_BMC_nterm_sig_pep_reverse | 100 | 68.717 | 54.025 | TTTTTGGTCTCAGCACTATGTTTAAAACCTCATTGATTATTGTTCTAATAAAGCGTATTTTCCATATGATATCTCTCTTAAAATTCACAAA |
| j5_00025_(GFPuv)_pure_forward | 31 | 60.539 | 60.539 | AAAGGAGAAGCACTTTCTACTGAGTTGTC |
| j5_00026_(long_gly_ser_linker)_GFPuv_forward | 92 | 80.194 | 60.539 | TTTTTGGTCTCAGTGGCAGTGTAGCGGAGCTCGGGTGGCTCAGGCTTGTTCCAGTAAAGGAGAAGCACTTTCTACTGAGTTGTC |

B

| Direct Synthesis Name | Alias | Contents | Length | Sequence |
|-----------------------|-------|---|--------|--------------|
| dsj5_00001 | | (BMC_nterm_sig_pep)_long_gly_ser_linker_(GFPuv)_ssrA_tag_5prime | 853 | GGAGATATACAT |

C

| PCR Reactions | Forward Oligo | Reverse Oligo | First Target Part | Last Target Part | Note | Mean Oligo Tm | Delta Oligo Tm | Mean Oligo Tm (3' only) | Delta Oligo Tm (3' only) | Length | Sequence |
|--|---------------|---------------|-------------------|------------------|-------|---------------|----------------|-------------------------|--------------------------|--------|--------------|
| 0 pS8c-gfpuv_sigpep | 0 j5_00001 | 2 j5_00003 | 0 | 0 | 0 PCR | 56.4505 | 4.851 | 56.4505 | 4.851 | 4852 | TAAATCGAGTAA |
| 1 pS8c-gfpuv_sigpep | 4 j5_00005 | 6 j5_00007 | 3 | 3 | 3 PCR | 62.919 | 4.76 | 62.919 | 4.76 | 711 | AAAGGAGAAGAA |
| 2 PCR/SOE Reaction 0 pS8c-gfpuv_sigpep | 1 j5_00002 | 3 j5_00004 | 4 | 1 | 1 PCR | 73.348 | 5.546 | 56.4505 | 4.851 | 4621 | GCCCAACGATGA |
| 3 PCR/SOE Reaction 1 pS8c-gfpuv_sigpep | 5 j5_00006 | 7 j5_00008 | 2 | 2 | 4 PCR | 78.8955 | 1.031 | 62.919 | 4.76 | 809 | CAATGAAGTTT |

D

| Assembly Pieces (SLIC/Gibson/CPEC) | PCR ID Number | First Target Part | Core Target Part | Last Target Part | CPEC Tm Previous (3' only) | CPEC Tm Next (3' only) | Overlap with Previous (bps) | Overlap with Next (bps) | Length | Sequence |
|------------------------------------|---------------|-------------------|------------------|------------------|----------------------------|------------------------|-----------------------------|-------------------------|--------|--------------|
| 0 PCR | 2 | 5 | 0 | 1 | 62.805 | 61.36 | 26 | 39 | 4621 | GCCCAACGATGA |
| 1 PCR | 3 | 2 | 3 | 4 | 60.083 | 62.805 | 39 | 26 | 809 | CAATGAAGTTT |

E

| Assembly Pieces (Golden-gate) | PCR ID Number | First Target Part | Core Target | Last Target | Overhang with Previous | Overhang with Next | Relative Overhang Position | Length | Sequence |
|-------------------------------|---------------|-------------------|-------------|-------------|------------------------|--------------------|----------------------------|--------|--------------|
| 0 PCR | 2 | 5 | 0 | 1 | AACT | GGTG | 2 | 4621 | TTTTTTGGTCTC |
| 1 PCR | 3 | 2 | 3 | 4 | GGTG | AACT | 2 | 804 | TTTTTTGGTCTC |

F

| Combinations of Assembly Pieces | Bin 0 | Bin 1 |
|---------------------------------|---|---|
| Variant | Assembly Method | Assembly Piece ID Number |
| Number | Part(s) | Part(s) |
| 0 | pj5_00003 Golden-gate (ssrA_tag_3prime) (pNJH0010_vector_backbone) (BMC_nterm_sig_pep) | 0 (long_gly_ser_linker) (GFPuv) (ssrA_tag_5prime) |
| 1 | pj5_00004 Golden-gate (ssrA_tag_3prime) (pNJH0010_vector_backbone) (BMC_nterm_sig_pep) | 0 (long_gly_ser_linker) (GFPuv) (ssrA_tag_enhanced_5prime) |
| 2 | pj5_00005 Golden-gate (ssrA_tag_3prime) (pNJH0010_vector_backbone) (BMC_nterm_sig_pep) | 0 (short_gly_ser_linker) (GFPuv) (ssrA_tag_5prime) |
| 3 | pj5_00006 Golden-gate (ssrA_tag_3prime) (pNJH0010_vector_backbone) (BMC_nterm_sig_pep) | 0 (short_gly_ser_linker) (GFPuv) (ssrA_tag_enhanced_5prime) |
| 4 | pj5_00007 Golden-gate (ssrA_tag_3prime) (pNJH0010_vector_backbone) (ccmN_nterm_sig_pep) | 5 (long_gly_ser_linker) (GFPuv) (ssrA_tag_5prime) |
| 5 | pj5_00008 Golden-gate (ssrA_tag_3prime) (pNJH0010_vector_backbone) (ccmN_nterm_sig_pep) | 5 (long_gly_ser_linker) (GFPuv) (ssrA_tag_enhanced_5prime) |
| 6 | pj5_00009 Golden-gate (ssrA_tag_3prime) (pNJH0010_vector_backbone) (ccmN_nterm_sig_pep) | 5 (short_gly_ser_linker) (GFPuv) (ssrA_tag_5prime) |
| 7 | pj5_00010 Golden-gate (ssrA_tag_3prime) (pNJH0010_vector_backbone) (ccmN_nterm_sig_pep) | 5 (short_gly_ser_linker) (GFPuv) (ssrA_tag_enhanced_5prime) |

G

| Plasmid Name | Alias | Contents | Length | Sequence |
|--------------|-------|--|--------|--------------|
| pj5_00001 | | (pBBS8c-RFP_EcoRI_XhoI_vector_backbone) (RBS) (gfpuv_sigpep_5prime) (gfpuv_sigpep_XhoI_silent) (gfpuv_sigpep_middle) (gfpuv_sigpep_BamHI_silent) (gfpuv_sigpep_3prime) | 5299 | GAGCTCTTATGA |
| pj5_00002 | | (pS8c-gfpuv_sig_pep_vector_backbone) (umuD_tag) | 5422 | GACCTCTTATGA |
| pj5_00003 | | (pS8c-vector_backbone)_BMC_nterm_sig_pep (long_gly_ser_linker) (GFPuv) (ssrA_tag_5prime) (ssrA_tag_3prime) | 5365 | TCATTTTCGCCA |
| pj5_00004 | | (pS8c-vector_backbone) (BMC_nterm_sig_pep) (long_gly_ser_linker) (GFPuv) (ssrA_tag_enhanced_5prime) (ssrA_tag_3prime) | 5371 | TCATTTTCGCCA |
| pj5_00005 | | (pS8c-vector_backbone) (BMC_nterm_sig_pep) (short_gly_ser_linker) (GFPuv) (ssrA_tag_5prime) (ssrA_tag_3prime) | 5341 | TCATTTTCGCCA |
| pj5_00006 | | (pS8c-vector_backbone) (BMC_nterm_sig_pep) (short_gly_ser_linker) (GFPuv) (ssrA_tag_enhanced_5prime) (ssrA_tag_3prime) | 5347 | TCATTTTCGCCA |
| pj5_00007 | | (pS8c-vector_backbone) (ccmN_nterm_sig_pep) (long_gly_ser_linker) (GFPuv) (ssrA_tag_5prime) (ssrA_tag_3prime) | 5371 | TCATTTTCGCCA |
| pj5_00008 | | (pS8c-vector_backbone) (ccmN_nterm_sig_pep) (long_gly_ser_linker) (GFPuv) (ssrA_tag_enhanced_5prime) (ssrA_tag_3prime) | 5377 | TCATTTTCGCCA |
| pj5_00009 | | (pS8c-vector_backbone) (ccmN_nterm_sig_pep) (short_gly_ser_linker) (GFPuv) (ssrA_tag_5prime) (ssrA_tag_3prime) | 5347 | TCATTTTCGCCA |
| pj5_00010 | | (pS8c-vector_backbone) (ccmN_nterm_sig_pep) (short_gly_ser_linker) (GFPuv) (ssrA_tag_enhanced_5prime) (ssrA_tag_3prime) | 5353 | TCATTTTCGCCA |

Figure S3. Example j5 output. Zoom in with PDF display software as desired to improve legibility. **(A)** Example master oligos list CSV input file, stylized for clarity. The user may specify the names (first column), lengths (in bp, second column), full-length (third column) and template-annealing 3' end (fourth column) melting temperatures, and DNA sequences (fifth column) of oligos in the user's collection. Subsequent to the design process, j5 appends to this list the new oligo(s) to be ordered, following the naming and numbering convention the user specifies (first column). **(B)** Example master direct DNA syntheses list CSV input file, stylized for clarity. The user may specify the name (first column), alias (second column), contents (part names enclosed in parentheses separated by underscores; third column), length (in bp, fourth column), and DNA sequence (fifth column) of directly synthesized DNA sequences in the user's collection. Subsequent to the design process, j5 appends to this list the new direct synthesis sequence(s) to be ordered, following the naming and numbering convention used in the first column. **(C)** Example PCR Reactions section of an assembly design CSV output file, stylized for clarity. The primary (second column) and alternative (third column) templates, forward (fifth column) and reverse (seventh column) primers (as determined by Algorithm S2), full-length (mean, eleventh

column; delta, twelfth column) and template-annealing 3' end (mean, thirteenth column; delta, fourteenth column) primer melting temperatures, product length (in bp, fifteenth column) and sequence (sixteenth column), are shown for each PCR reaction. The parts contained within each PCR product (from first part, eighth column, to the last part, ninth column, corresponding to that shown in Figure S1F), and a note (tenth column) indicating whether the PCR product should be SOE'd together with adjacent assembly pieces prior to the DNA assembly process, are also shown for each PCR reaction. **(D-E)** Example Assembly Pieces section of an assembly design CSV output file, stylized for clarity. **(D)** SLIC/Gibson/CPEC assembly. The upstream (seventh column) and downstream (eighth column) flanking homology sequence melting temperatures, corresponding upstream (ninth column) and downstream (tenth column) flanking homology sequence overlap lengths, length (in bp, eleventh column) and sequence (twelveth column), are shown for each assembly piece. The parts contained (from first part, fourth column, to the last part, sixth column, corresponding to that shown in Figure S1F), derivation (e.g. PCR or digest; second column), and corresponding PCR reaction number (if applicable, third column, corresponding to that shown in (C) are also shown for each assembly piece. **(E)** Golden Gate assembly. The upstream (seventh column) and downstream (eighth column) top strand overhang sequences (as determined by Algorithm S4), and the downstream relative overhang position (in bp, ninth column; see Figure S2E), are shown for each assembly piece. Other columns are as in (D). **(F)** Example Combinations of Assembly Pieces section of an assembly design CSV output file, stylized for clarity. The assembly method (third column) and the assembly piece in each combinatorial bin corresponding to the variant (fourth and columns thereafter) is shown for each plasmid variant to be constructed (second column). **(G)** Example master plasmids list CSV input file, stylized for clarity. The user may optionally specify the names (first column), aliases (second column), contents (part names enclosed in parentheses separated by underscores, third column), lengths (in bp, fourth column), and DNA sequences (fifth column) of plasmids in the user's collection. Subsequent to the design process, j5 appends to this list the new plasmid(s) to be constructed, following the naming and numbering convention the user specifies (first column).

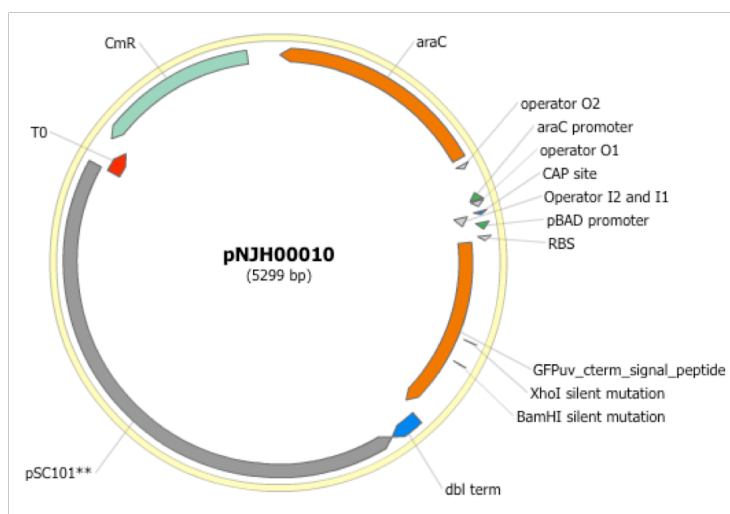


Figure S4. Plasmid map of pNJH00010 derived from the Genbank-format sequence file resulting from j5-designed SLIC/Gibson/CPEC assembly (Figure 2).

A

| PLATE ID | PLATE WELL | LIQUID TYPE | VOLUME (uL) |
|--------------|------------|--|-------------|
| oligos_plate | A01 | j5_00001_(gfpuv_sigpep_5prime)_pure_forward | 100 |
| oligos_plate | B01 | j5_00002_(RBS_(gfpuv_sigpep_5prime)_forward | 100 |
| oligos_plate | C01 | j5_00003_(gfpuv_sigpep_5prime)_pure_reverse | 100 |
| oligos_plate | D01 | j5_00004_(gfpuv_sigpep_5prime_(gfpuv_sigpep_XhoI_silent)_reverse | 100 |
| oligos_plate | E01 | j5_00005_(gfpuv_sigpep_middle)_pure_forward | 100 |
| oligos_plate | F01 | j5_00006_(gfpuv_sigpep_middle)_pure_forward | 100 |

B

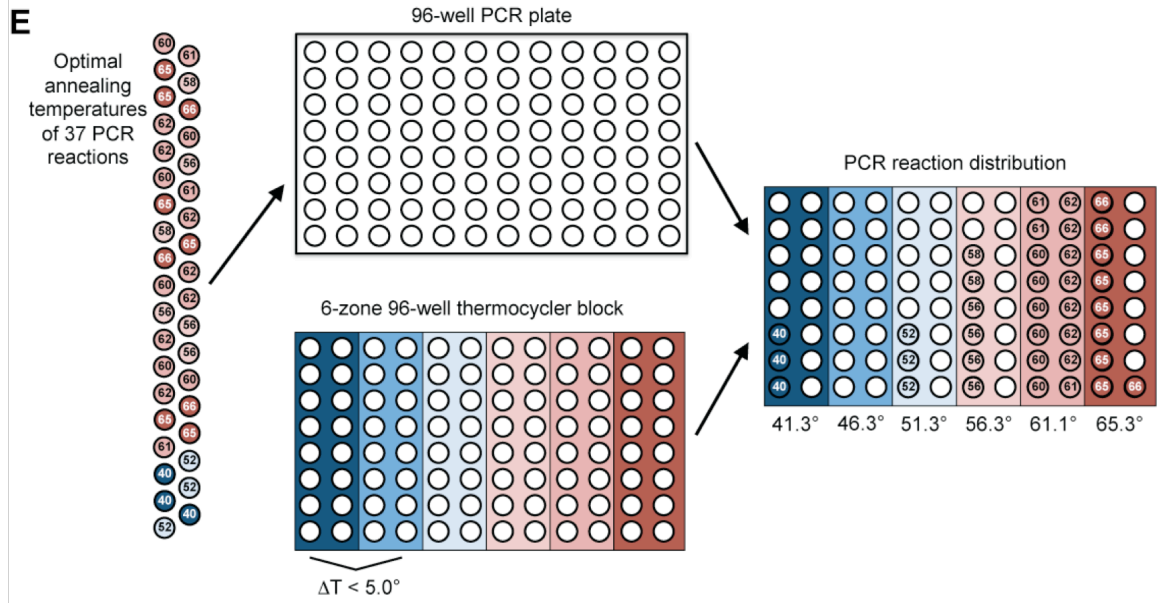
| Parameter Name | Value | Default Value | Description |
|--|--------|---------------|--|
| MAXDELTATEMPERATUREADJACENTBLOCKS | 5 | 5 | The maximum difference in temperature (in C) between adjacent zones on the thermocycler block |
| MAXDELTATEMPERATUREACTIVATIONTEMPERATURE | 1000 | 1000 | The maximum number of Monte-Carlo steps attempted per thermocycler block zone |
| MAXDELTATEMPERATURE | 100 | 100 | The maximum liquid volume (in uL) that a well in the multi-well plate can hold |
| MINTEMPERATUREFINAL | 0.0001 | 0.0001 | The final temperature at the end of the Monte-Carlo simulated annealing run (in arbitrary reduced units) |
| MINTEMPERATUREINITIAL | 0.1 | 0.1 | The initial temperature in the beginning of the Monte-Carlo simulated annealing run (in arbitrary reduced units) |
| MINTEMPERATURE | 5 | 5 | The minimum plating volume (in uL) for a robotic platform (in uL) |
| NUMCOLUMNSINWELLPLATE | 12 | 12 | The number of columns in the multi-well plate |
| NUMROWSINWELLPLATE | 8 | 8 | The number of rows in the multi-well plate |
| TRIALCOSTTEMPERATURE | 0.1 | 0.1 | The Monte-Carlo step trial change in temperature for a thermocycler block zone |
| WELLSPERTHERMOCYCLERBLOCK | 144 | 144 | The number of wells per thermocycler block zone |
| ZONESPERTHERMOCYCLERBLOCK | 6 | 6 | The number of zones per thermocycler block |

C

| ROW | TEMPLATE_PLATE | TEMPLATE_WELL | TEMPLATE_VOLUME | PRIMER1_PLATE | PRIMER1_WELL | PRIMER1_VOLUME | PRIMER2_PLATE | PRIMER2_WELL | PRIMER2_VOLUME | WATER_VOLUME | OUTPUT_PLATE | OUTPUT_WELL | REACTOR_NUMBER | OPTIMAL_ANNEALING_TEMP | THERMOCYCLER_BLOCK | THERMOCYCLER_ZONE | THERMOCYCLER_ZONE_ANNEALING_TEMP | EXPECTED_SIZE |
|-----|----------------|---------------|-----------------|---------------|--------------|----------------|---------------|--------------|----------------|--------------|--------------|-------------|----------------|------------------------|--------------------|-------------------|----------------------------------|---------------|
| 1 | oligos_plate | B01 | 100 | oligos_plate | B01 | 100 | oligos_plate | B01 | 100 | 100 | oligos_plate | B01 | 1 | 56 | 0 | 0 | 56 | 4000 |
| 2 | oligos_plate | B01 | 100 | oligos_plate | B01 | 100 | oligos_plate | B01 | 100 | 100 | oligos_plate | B01 | 2 | 57.5 | 0 | 0 | 57.5 | 4000 |
| 3 | oligos_plate | B01 | 100 | oligos_plate | B01 | 100 | oligos_plate | B01 | 100 | 100 | oligos_plate | B01 | 3 | 58.6 | 0 | 0 | 58.6 | 4000 |
| 4 | oligos_plate | B01 | 100 | oligos_plate | B01 | 100 | oligos_plate | B01 | 100 | 100 | oligos_plate | B01 | 4 | 59.2 | 0 | 0 | 59.2 | 4000 |
| 5 | oligos_plate | B01 | 100 | oligos_plate | B01 | 100 | oligos_plate | B01 | 100 | 100 | oligos_plate | B01 | 5 | 62.5 | 0 | 0 | 62.5 | 4000 |
| 6 | oligos_plate | B01 | 100 | oligos_plate | B01 | 100 | oligos_plate | B01 | 100 | 100 | oligos_plate | B01 | 6 | 63.8 | 0 | 0 | 63.8 | 4000 |

D Thermocycler Blocks:

| BLOCK ID | BLOCK_ZONE | BLOCK_ZONE_ANNEALING_TEMP |
|----------|------------|---------------------------|
| 0 | 0 | 56 |
| 0 | 1 | 57.5 |
| 0 | 2 | 58.6 |
| 0 | 3 | 59.2 |
| 0 | 4 | 62.5 |
| 0 | 5 | 63.8 |



F

| Index | control1 | TEMPLATE_VOLUME | control1_PRIMER1_VOLUME | control1_PRIMER2_VOLUME | TEMPLATE_PLATE | TEMPLATE_WELL | TEMPLATE_VOLUME | PRIMER1_PLATE | PRIMER1_WELL | PRIMER1_VOLUME | PRIMER2_PLATE | PRIMER2_WELL | PRIMER2_VOLUME | WATER_VOLUME | OUTPUT_PLATE | OUTPUT_WELL |
|-------|----------|-----------------|-------------------------|-------------------------|----------------|---------------|-----------------|---------------|--------------|----------------|---------------|--------------|----------------|--------------|--------------|-------------|
| 1 | Normal | Normal | Normal | Normal | oligos_plate | 2 | 5 | oligos_plate | 21 | 5 | oligos_plate | 23 | 5 | 0 | oligos_plate | 23 |
| 2 | Normal | Normal | Normal | Normal | oligos_plate | 2 | 5 | oligos_plate | 22 | 5 | oligos_plate | 24 | 5 | 0 | oligos_plate | 24 |
| 3 | Normal | Normal | Normal | Normal | oligos_plate | 2 | 5 | oligos_plate | 23 | 5 | oligos_plate | 25 | 5 | 0 | oligos_plate | 25 |
| 4 | Normal | Normal | Normal | Normal | oligos_plate | 2 | 5 | oligos_plate | 24 | 5 | oligos_plate | 26 | 5 | 0 | oligos_plate | 26 |
| 5 | Normal | Normal | Normal | Normal | oligos_plate | 1 | 5 | oligos_plate | 13 | 5 | oligos_plate | 15 | 5 | 0 | oligos_plate | 15 |
| 6 | Normal | Normal | Normal | Normal | oligos_plate | 1 | 5 | oligos_plate | 14 | 5 | oligos_plate | 16 | 5 | 0 | oligos_plate | 16 |
| 7 | Normal | Normal | Normal | Normal | oligos_plate | 2 | 5 | oligos_plate | 13 | 5 | oligos_plate | 17 | 5 | 0 | oligos_plate | 17 |
| 8 | Normal | Normal | Normal | Normal | oligos_plate | 1 | 5 | oligos_plate | 14 | 5 | oligos_plate | 18 | 5 | 0 | oligos_plate | 18 |
| 9 | Normal | Normal | Normal | Normal | oligos_plate | 1 | 5 | oligos_plate | 15 | 5 | oligos_plate | 19 | 5 | 0 | oligos_plate | 19 |
| 10 | Normal | Normal | Normal | Normal | oligos_plate | 2 | 5 | oligos_plate | 14 | 5 | oligos_plate | 20 | 5 | 0 | oligos_plate | 20 |
| 11 | Normal | Normal | Normal | Normal | oligos_plate | 2 | 5 | oligos_plate | 15 | 5 | oligos_plate | 21 | 5 | 0 | oligos_plate | 21 |
| 12 | Normal | Normal | Normal | Normal | oligos_plate | 2 | 5 | oligos_plate | 16 | 5 | oligos_plate | 22 | 5 | 0 | oligos_plate | 22 |
| 13 | Normal | Normal | Normal | Normal | oligos_plate | 2 | 5 | oligos_plate | 17 | 5 | oligos_plate | 23 | 5 | 0 | oligos_plate | 23 |
| 14 | Normal | Normal | Normal | Normal | oligos_plate | 2 | 5 | oligos_plate | 18 | 5 | oligos_plate | 24 | 5 | 0 | oligos_plate | 24 |
| 15 | Normal | Normal | Normal | Normal | oligos_plate | 2 | 5 | oligos_plate | 19 | 5 | oligos_plate | 25 | 5 | 0 | oligos_plate | 25 |
| 16 | Normal | Normal | Normal | Normal | oligos_plate | 2 | 5 | oligos_plate | 20 | 5 | oligos_plate | 26 | 5 | 0 | oligos_plate | 26 |
| 17 | Normal | Normal | Normal | Normal | oligos_plate | 3 | 5 | oligos_plate | 17 | 5 | oligos_plate | 19 | 5 | 0 | oligos_plate | 19 |
| 18 | Normal | Normal | Normal | Normal | oligos_plate | 3 | 5 | oligos_plate | 18 | 5 | oligos_plate | 20 | 5 | 0 | oligos_plate | 20 |

Figure S5. Example multi-well plate j5 input and output. Zoom in with PDF display software as desired to improve legibility. **(A)** Example multi-well plate CSV input file, stylized for clarity. The user must specify the volume (in μL ; fourth column) for each liquid component (third column) for each well (second column) for each plate that will be utilized in the DNA assembly process. **(B)** Example downstream automation parameters CSV input file, stylized for clarity. Default values (third column) and descriptions (fourth column) are provided as a reference for each parameter name (first column). The user may change parameter values by modifying the entries in the second column. **(C)** PCR Reactions section of a distribute PCR reactions CSV output file, stylized for clarity. The plate (second column), well (third column), and volume (in μL ; fourth column) of each template; the plate (fifth column), well (sixth column), and volume (in μL ; seventh column) of each forward primer; the plate (eighth column), well (ninth column), and volume (in μL ; tenth column) of each reverse primer; the

volume of water to be added (eleventh column); the destination plate (twelfth column) and well (thirteenth column); the optimal annealing temperature (fifteenth column); the destination thermocycler block (sixteenth column), zone (seventeenth column), and annealing temperature (eighteenth column); and the expected product size (in bp, nineteenth column) are shown for each PCR reaction (fourteenth column, corresponding to that shown in Figure S3C). **(D)** Thermocycler Blocks section of a distribute PCR reactions CSV output file, stylized for clarity. The annealing temperature (third column) for each zone (second column) in each thermocycle block (first column). **(E)** Optimal distribution of PCR reactions across thermo-cycler annealing temperature gradients. Given the optimal annealing temperatures of each of the PCR reactions required for an assembly process and the thermocycler block gradient constraints (e.g. each neighboring zone must differ by less than 5 °C, as shown, see (B)), j5 optimizes the thermocycler block annealing temperature gradient(s), and distributes the PCR reactions across multi-well plate(s) that will be placed in these optimized gradient(s). **(F)** NextGen (eXeTek) Expression workstation control CSV output file, stylized for clarity. The NextGen-specific template (second column), forward primer (third column), and reverse primer (fourth column) control parameters; the plate (fifth column), well index (sixth column), and volume (in μL ; seventh column) of each template; the plate (eighth column), well index (ninth column), and volume (in μL ; tenth column) of each forward primer; the plate (eleventh column), well index (twelfth column), and volume (in μL ; thirteenth column) of each reverse primer; the volume of water to be added (fourteenth column); and the destination plate (fifteenth column) and well index (sixteenth column) are shown for each PCR reaction.

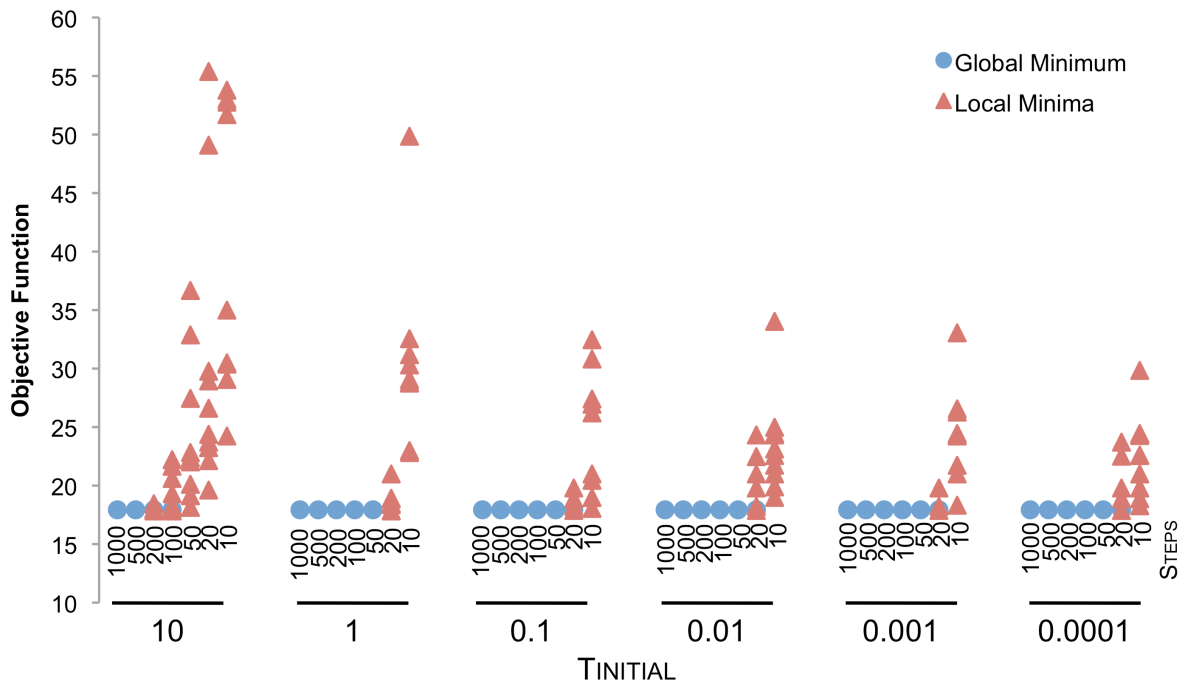


Figure S6. Algorithm S5 convergence as a function of MAXMCSTEPSPERZONE and MCTEMPERATUREINITIAL parameters for the PCR reactions shown in Figure S5E. Algorithm S5 was run 10 times for each choice of MAXMCSTEPSPERZONE (here “STEPS”) and MCTEMPERATUREINITIAL (here “TINITIAL”), with all other parameters set to their respective j5 default values. The best objective function encountered for each run is plotted with either a red triangle indicating a non-global minima, or a blue circle indicating the global minimum. All runs with 50 or more MAXMCSTEPSPERZONE (with the exception of MCTEMPERATUREINITIAL = 10, which required 500 or more MAXMCSTEPSPERZONE) identified the global minimum. The default parameters for j5 are MCTEMPERATUREINITIAL = 0.1 and MAXMCSTEPSPERZONE = 1000.

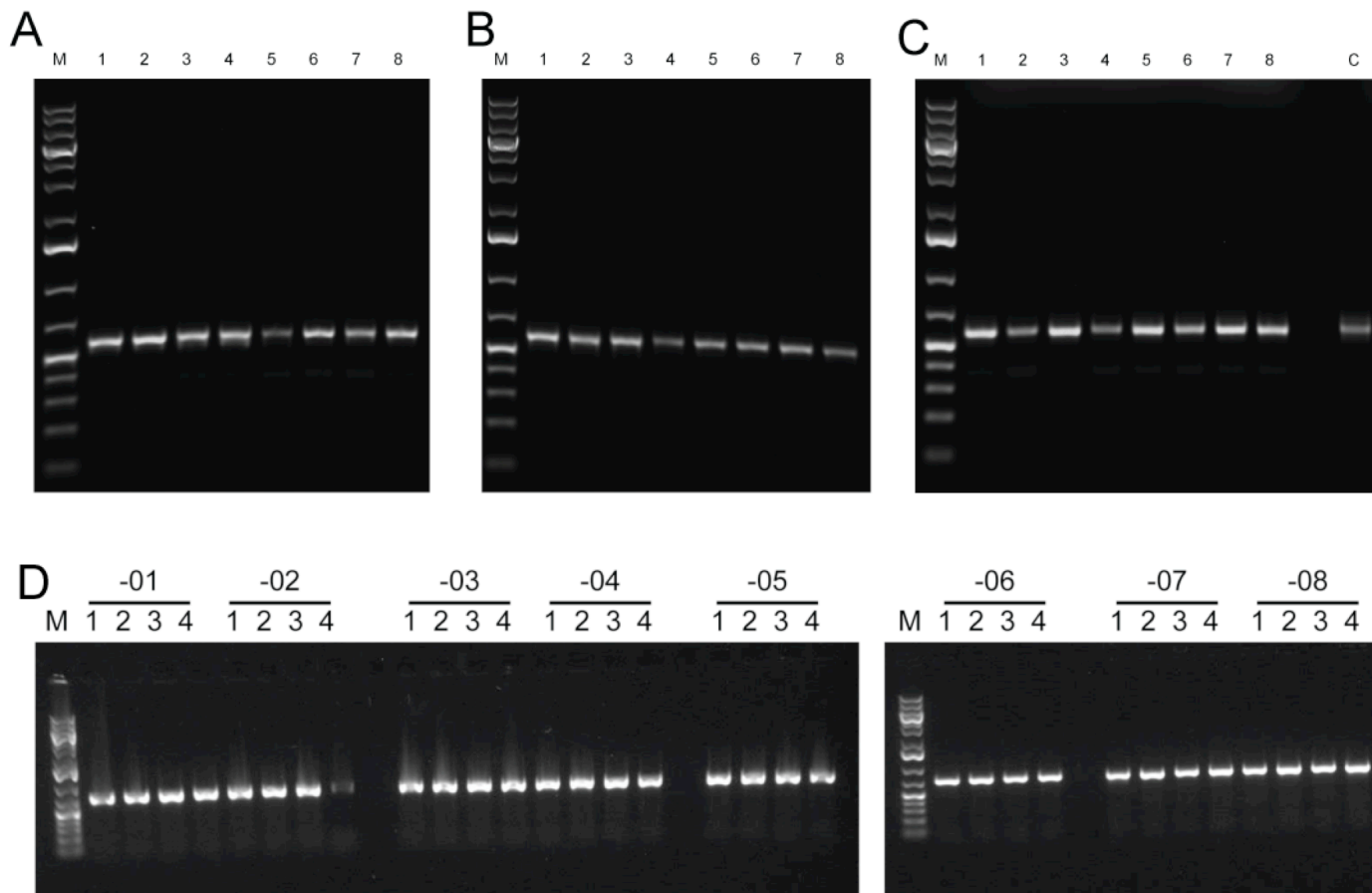


Figure S7. Colony PCR screening. **(A-C)** Colony PCR screening of pNJH00010 transformants of **(A)** CPEC, **(B)** Gibson, and **(C)** SLIC assemblies. **(A-C)** Lane 1 – 1 kb+ DNA ladder “M”; lanes 2 through 9 – amplicons from colonies “1” through “8” (respectively). **(C)** Lane 11 – plasmid DNA positive control “C”. **(D)** Agarose gel electrophoresis of colony PCRs of combinatorial Golden Gate assembly transformants. Four colonies were screened for each transformation of plasmids pRDR00001 - pRDR00008 (indicated as -01, -02, -03, ... -08). Lane 1 – 1 kb+ DNA ladder “M”.

C. ecRDR10003

5' 3' ΔclpX genomic locus

Markerless knockout



B. ecRDR10002

Intermediate genomic insertion



A. ecRDR10001

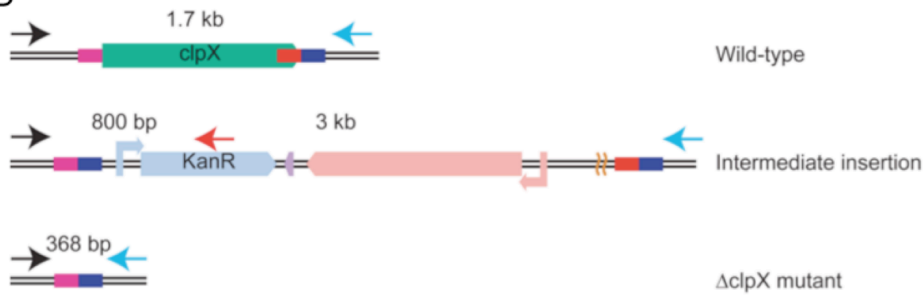
5' 3' H1 clpX H2H3 Wild-type genomic locus

λ-red mediated homologous recombination between flanking H1 and H2 motifs.



PCR amplification using pSKI primers with flanking genomic homology sequences

D



E

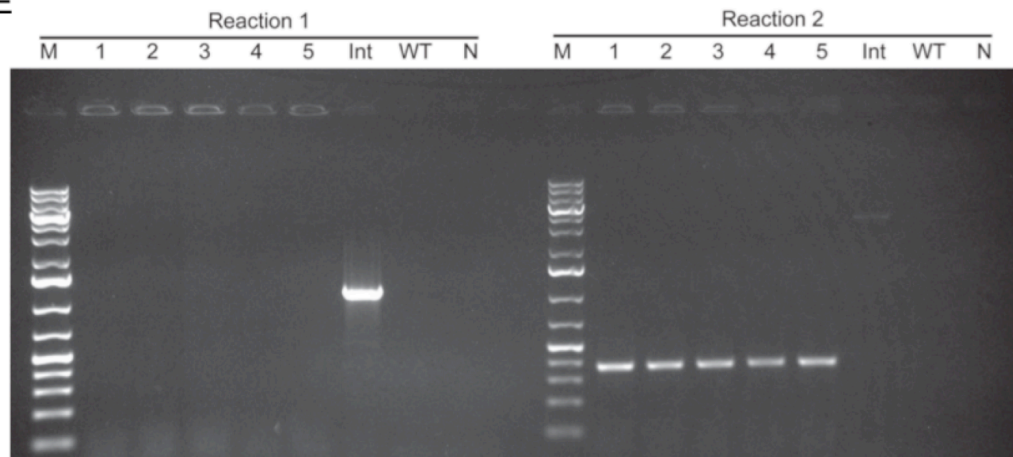


Figure S8. *clpX* deletion. **(A-B)** *clpX* deletion cassette design. **(A)** Schematic of the linear *clpX* deletion cassette (JPUB_000255) assembly task. The deletion cassette region from plasmid pSKI (7), spanning from the promoter region upstream of *kanR* through the I-SceI homing-endonuclease recognition sequence is PCR amplified, with the forward primer introducing a sequence homologous to the *E. coli* genome immediately upstream of the *clpX* coding sequence (H1) and a sequence homologous to the genome immediately downstream of the *clpX* coding sequence (H3), and the reverse primer introducing a sequence homologous to a portion of *clpX* coding sequence (H2). **(B)** Schematic of the marker-less deletion of the genomic copy of *clpX* utilizing the linear deletion cassette. The deletion cassette depicted in (A) is transformed into *E. coli* (strain ecRDR10001/JBEI-2948) expressing the λ -red recombinase system from plasmid pREDI (7). Following λ -red mediated double-homologous recombination (at the H1 and H2 loci), replacing *clpX* in situ with the deletion cassette, transformant colonies are selected from kanamycin agar plates (strain ecRDR10002/JBEI-3080). Following the expression of the I-SceI homing-endonuclease from the pREDI plasmid, double stranded break at the I-SceI recognition site within the deletion cassette, and homologous recombination at the H3 locus, colonies are selected from sucrose (*sacB* counter-selection) agar plates, and counter-screened for kanamycin sensitivity, indicating the markerless deletion of *clpX* (strain ecRDR10003/JBEI-3083). **(D-E)** Colony PCR *clpX* protease deletion validations. **(D)** Schematic of diagnostic colony PCR reactions. Reaction 1: forward primer (black arrows) anneals to sequence flanking the 5' end of the *clpX* coding sequence (CDS), reverse primer (red arrow) anneals within the *kanR* CDS. Reaction 1 should result in an 800 bp product for the *clpX* deletion cassette integration intermediate, but in no product for $\Delta clpX$ mutant nor wildtype. Reaction 2: forward primer (black arrows) anneals to sequence flanking the 5' end of the *clpX* CDS, reverse primer (blue arrows) anneals to sequence flanking the 3' end of the *clpX* CDS. Reaction 2 should result in a 368 bp product for a $\Delta clpX$ mutant, a 3 kb product for the *clpX* deletion cassette integration intermediate, or a 1.7 kb product for WT. **(E)** Colony PCR validations of *clpX* markerless deletion (JBEI-3083). For each reaction 1 and reaction 2: Lane 1 – 1kb DNA ladder “M”, lanes 2 through 6 – $\Delta clpX$ mutants 1 through 5 (respectively), lane 7 – *clpX* deletion cassette integration intermediate (strain JBEI-3080), lane 8 – WT control (JBEI-2948), lane 9 – no DNA template control. All bands were observed at the expected size. In reaction 2, the integration intermediate band is faint but present, while the expected wildtype band was not detected.

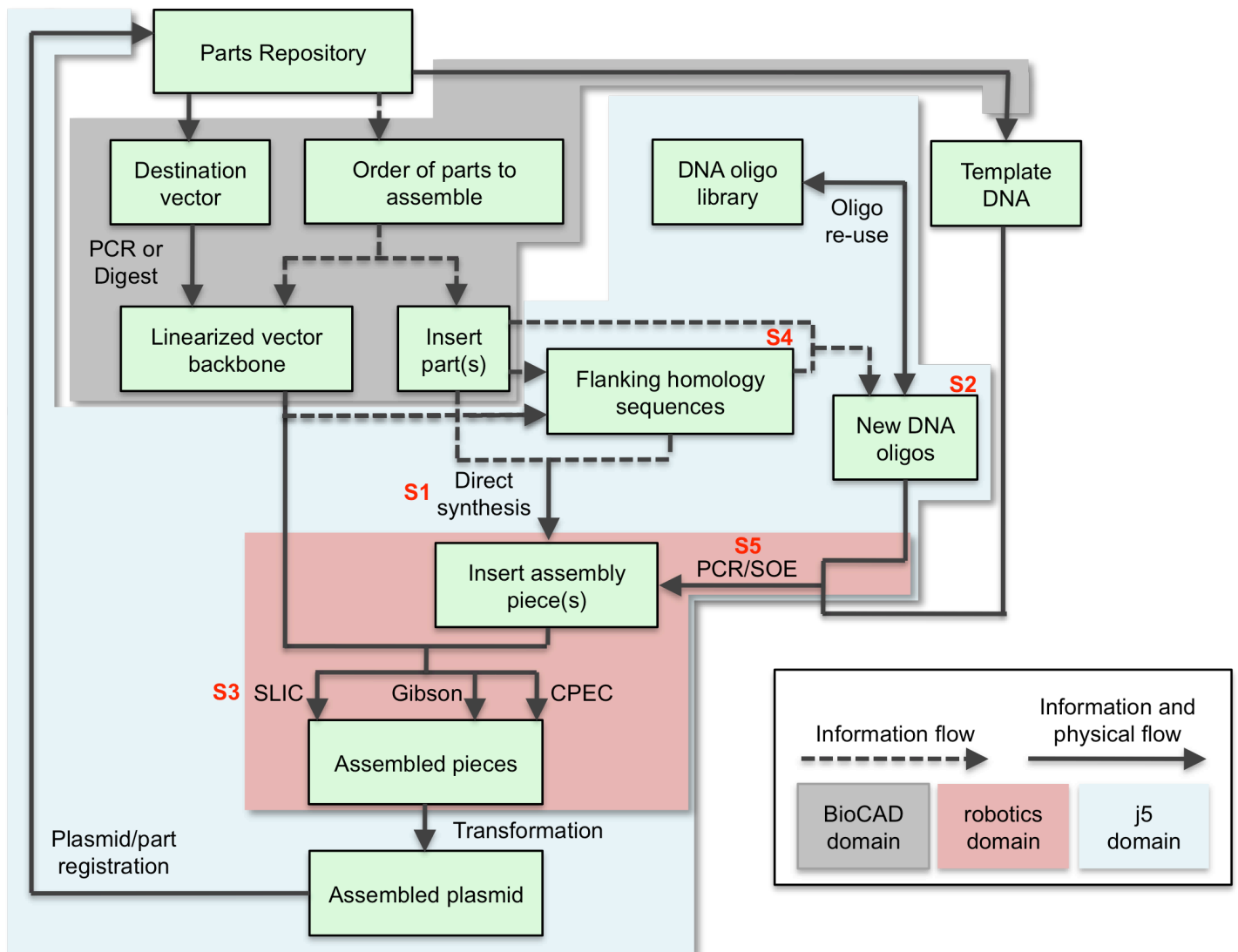


Figure S9. Detailed workflow for SLIC/Gibson/CPEC assembly. A researcher begins the DNA assembly process by selecting parts to assemble from a registry of biological parts (such as the JBEI-ICE repository) or a local collection of DNA sequences; biological computer-aided design (BioCAD) tools may assist this process. The parts to assemble are categorized into either the linearized destination vector, or insert parts. The linearized destination vector is physically achieved by digesting the destination vector with restriction enzymes (as in Figure 2) or by PCR-amplifying the vector backbone (as in Figure 3). Given the sequences of the linearized destination vector and the insert parts, j5 designs flanking homology sequences for each assembly piece, and performs an analysis to determine for which (if any) portions of the assembly direct synthesis would be more cost-effective than either PCR/SOE or oligo embedding. j5 then designs DNA oligos for synthesis, and/or suggests re-use of existing oligos where possible, to amplify the desired assembly pieces. The parts to be assembled do not need to physically exist before using j5 to design the assembly, since it is possible to specify a direct synthesis strategy for any assembly fragment. Liquid handling robotics or other devices may assist the execution of PCR/SOE to generate the assembly pieces, as well as their subsequent SLIC/Gibson/CPEC assembly. j5 facilitates this process by condensing/aggregating designs for multiple independent assemblies into 96-well plate format including optimally distributing reactions across a thermocycler annealing temperature gradient (as in Figure S5E). After transforming a competent cloning strain with the assembly reaction, a clonal isolate of the assembled plasmid is sequence verified, assayed for function as desired, and then deposited into the parts registry or local collection for subsequent re-use. The Golden Gate process is analogous that shown, with the design of overhang sequences substituting for the design of flanking homology sequences. S1-S5 (bold red lettering) refer to locations within the workflow where Algorithms S1-S5 are utilized. Algorithm S1 determines when DNA synthesis is cost-effective, S2 assists the design of new DNA oligos, S3 determines if a hierarchical assembly strategy is required, S4 optimizes the design of Golden Gate overhang sequences, and S5 optimizes the placement of PCR reactions across thermocycler gradients.

ALGORITHMS

Algorithm S1: After the user has selected an assembly methodology (SLIC/Gibson/CPEC or Golden Gate), heuristically determine the most cost-effective strategy to incorporate each part into an assembly fragment prior to executing the full assembly design process.

```
1:  for all part ∈ part_list do
2:      if not defined part.strategy then
3:          if part.length < minimum_PCR_length then
4:              if CanEmbedInPrimer(part) then
5:                  part.strategy ← embed_in_primer
6:              else
7:                  part.strategy ← synthesis
8:              end if
9:          else
10:             part.strategy ← PCR
11:          end if
12:      end if
13:  end for
14:  for all part ∈ part_list do
15:      if part.strategy ≠ synthesis then
16:          if MarginalPCRCost(part) > SynthesisCost(part) then
17:              part.strategy ← synthesis
18:          end if
19:      end if
20:  end for
21:  for all part ∈ part_list do
22:      if part.strategy = synthesis then
23:          if part.next.strategy ≠ synthesis then
24:              if MarginalPCRCost(part.next) > MarginalSynthesisCost(part.next) then
25:                  part.next.strategy ← synthesis
26:              end if
27:          end if
28:      end if
29:  end for
30:  for all part ∈ part_list do
31:      if part.strategy = synthesis then
32:          if part.previous.strategy ≠ synthesis then
33:              if MarginalPCRCost(part.previous) > MarginalSynthesisCost(part.previous) then
34:                  part.previous.strategy ← synthesis
35:              end if
36:          end if
37:      end if
38:  end for
```

where MarginalPCRCost() returns the (in context) marginal cost of adding the part to its designated PCR reaction;

where MarginalSynthesisCost() returns the (in context) marginal cost of adding the part to the adjacent direct synthesis fragment.

Direct synthesis orders often have minimum charges per synthesized sequence (e.g. \$0.39/bp and a \$159 minimum per sequence), so the marginal cost of adding a part to an adjacent direct synthesis fragment might be significantly less expensive than directly synthesizing the part by itself (since an additional minimum charge will not be incurred). This is the justification for the third step of Algorithm S1. Algorithm S1 assumes that the

most likely primer lengths, and flanking sequence lengths (SLIC, Gibson or CPEC) or relative overhang positions (Golden Gate) will be used throughout the assembly process. Since primer, flanking sequence, and relative overhang positions are optimized during the design process and thereby differ from the most likely values, this heuristic may fail at non-continuities in the MarginalPCRCost() function. For example, extending the length of a primer from 60 to 61 bp may result in an abrupt additional DNA oligo PAGE-purification cost which may be as much as an additional \$60/primer. For this reason, further development will focus on integrating the determination of the most cost-effective assembly strategy into the full design process.

Algorithm S1 is currently utilized after the user has already selected an assembly methodology. Further development of Algorithm S1 could assist the user in deciding which assembly method to select by comparing the cost and time requirements for the various assembly methods. This could include a refined distinction between SLIC, Gibson, and CPEC assembly from a method cost-perspective, associating differential anticipated failure rate risks as costs embodied in extra time, labor and DNA sequencing requirements. Furthermore, Algorithm S1 provides a reasonable heuristic for determining the most cost-effective assembly strategy for a single construct, but does not properly account for part re-use across a combinatorial library. For example, it may be less expensive to directly synthesize two parts in a single contiguous fragment (due to a minimum per sequence charge as described above). However, if each of the two parts can be repeatedly re-used across a combinatorial library, but the concatenation of the two parts is only used in one of the combinations, synthesizing the two parts separately can be effectively amortized over multiple combinations and provide the most cost-effective strategy. Further development will target combinatorial amortization accounting. In the meantime, a manual software control mechanism (direct synthesis firewalling) is in place that allows the user to prevent directly synthesizing adjacent parts together across combinatorial assembly junctions. Algorithm S1 does not account for the costs of enzymatic reagents, competent cells, sequencing reactions, nor labor charges (which may dominate in industry). Further development will target a more sophisticated cost function that includes these factors. Finally, j5 outputs only the Algorithm S1-calculated cost-optimal strategy, but could be further developed to provide a set of comparable alternatives when the difference in cost falls within a user-specifiable threshold.

Algorithm S2: Progressively relieve violated constraints during primer (or flanking sequence) design.

Existing programs such as Primer3 (11) can be successfully leveraged to optimize the design of primers or flanking homology sequences (effectively primers for adjacent assembly pieces during Gibson and CPEC assembly). One drawback to these existing software packages is that they provide primer pair designs only if a given set of design criteria is met. For example, if all considered primers fall outside of a desired melting temperature range, an error message is issued, but no primer designs are returned. While it may be possible to force the software to design at least one (if sub-optimal) primer pair per desired PCR reaction, this may result in many undesirable design constraint violations, even if primer pairs with fewer constraint violations (but perhaps with lower overall design scores, constraint violations aside) are accessible. Algorithm S2 first attempts to design optimal primers that meet all design constraints; if unable to do so, constraints are progressively relieved until an acceptable primer pair has been achieved. In addition to the primers (or flanking homology sequences) designed, warning messages are issued if any design constraints were violated/relieved during the design process and/or if any putative template mis-priming events with above threshold melting temperatures are identified via BLAST (12).

```
1: constraints ← target
2: repeat
3:   primers ← DesignPrimers(constraints)
4:   constraints.gc_clamp ← constraints.gc_clamp - 1
5: until defined primers or constraints.gc_clamp < 0
6: constraints.gc_clamp ← constraints.gc_clamp + 1
7: if not defined primers then
8:   repeat
9:     EliminateFirstViolatedConstraint(constraints)
10:    primers ← DesignPrimers(constraints)
11:   until defined primers
12: end if
13: while defined primers and constraints.gc_clamp < target.gc_clamp do
```

```

14:   constraints.gc_clamp ← constraints.gc_clamp + 1
15:   primers ← DesignPrimers(constraints)
16: end while
17: if not defined primers then
18:   constraints.gc_clamp ← constraints.gc_clamp - 1
19:   primers ← DesignPrimers(constraints)
20: end if

```

where DesignPrimers() returns the optimal primer pair if the design constraints can be met;

where EliminateFirstViolatedConstraint() identifies (via a rank-ordered triage process) the next violated constraint to relieve; the constraint rank-ordering (first eliminated to last) is as follows: too many Ns, too many poly-X, GC content, minimum T_m, maximum T_m, maximum difference in T_m, self-complementarity, and pair-complementarity.

For the SLIC/Gibson/CPEC design shown in Figure 2, of the 6 primers (required for the 3 PCR reactions) and the 6 PCR-derived assembly junction termini, only the 4 primers for PCR reactions “1” and “3” could be successfully designed by Primer3 without Algorithm S2 constraint relief. For this design, the particular rank-ordering of constraint relief had no impact on the total number or type of constraints relieved. For the combinatorial Golden Gate design shown in Figure 3, of the 12 primers required for the 6 PCR reactions, the 8 primers for PCR reactions “1”, “2”, “3”, and “4” could be successfully designed by Primer3 without Algorithm S2 constraint relief. Here too, the particular rank-ordering of constraint relief had no impact on the total number or type of constraints relieved. For other designs, the particular rank-ordering of constraint relief may have a more significant impact. Algorithm S2’s constraint rank-ordering is currently subjective. Over time, given an accumulated data set of PCR successes and failures, it would be possible to objectively analyze the relationship between relaxed constraint type and PCR or SLIC/Gibson/CPEC assembly failure rate.

It should be pointed out that (at least for Primer3), GC clamp length is associated only with a constraint, unlike primer melting temperature, for example, for which there are constraints (e.g. maximum and minimum acceptable temperature) in addition to a scoring function (distance from the target melting temperature) that rank-orders multiple putative primers that fall within constraint tolerances. As a consequence, no GC clamp is considered equivalent to a one or two-bp GC clamp if they are all shorter than the design constraint. For this reason, Algorithm S2 treats the GC clamp separately from all other constraints that have associated scoring functions; other constraint-only parameters could be similarly treated.

Algorithm S3: Identify SLIC/Gibson/CPEC assembly piece incompatibilities; if found, design a hierarchical assembly strategy

The SLIC (3), Gibson (2), and CPEC (4) assembly methodologies utilize sequence homology at assembly piece termini to direct the assembly process. If two or more assembly pieces have sufficiently identical sequence at their respective termini (e.g. fragments “2” and “5” in Figure S2A), there is an ambiguity in the assembly process, which can lead to undesirable products (e.g. pieces assembled in the incorrect order or sections missing altogether). These assembly pieces are said to be incompatible with one another, since placing them into the same assembly reaction can lead to undesired products. For the CPEC method in particular, and potentially for the Gibson method, there is an additional concern that the terminus of an assembly piece will mis-prime an internal portion of itself or another assembly piece (e.g. the 3’ end of fragment “4” could mis-prime the *P_{lac}* subsequence “4” in fragment “0” in Figure S2A), which can also lead to undesired assembly products. Algorithm S3 first identifies any putative assembly piece incompatibilities, and then attempts to design a hierarchical assembly strategy that mitigates the risk of incorrect assembly products. If no such hierarchical assembly strategy is possible, a warning message is issued.

```

1: for all start_piece ∈ piece_list do
2:   contig ← new Contig
3:   piece ← start_piece
4:   while piece.next ≠ start_piece and Compatible(contig, piece.next)
5:     push contig piece.next
6:     piece ← piece.next

```

```

7:   end while
8:   push contig_list contig
9: end for
10: EliminateEmptyOrSubsetContigs(contig_list)
11:   for all contig ∈ contig_list do
12:     for all piece ∈ contig do
13:       unique ← true
14:       for all other_contig ∈ contig_list and contig ≠ other_contig do
15:         if Contains(other_contig, piece) then
16:           unique ← false
17:         last
18:       end if
19:     end for
20:     if unique then
21:       for all other_contig ∈ contig_list and contig ≠ other_contig do
22:         for all other_piece ∈ contig do
23:           Remove(other_contig, other_piece)
24:         end for
25:       end for
26:     end if
27:   end for
28: end for
29: EliminateEmptyOrSubsetContigs(contig_list)
30:   for all contig ∈ contig_list do
31:     for all piece ∈ contig do
32:       for all other_contig ∈ contig_list and contig ≠ other_contig do
33:         Remove(other_contig, piece)
34:       end for
35:     end for
36: end for
37: EliminateEmptyOrSubsetContigs(contigs_list)
38: failure ← false
39:   for all contig ∈ contig_list do
40:     compatible ← false
41:     while not failure and not compatible do
42:       for all other_contig ∈ contig_list and contig ≠ other_contig do
43:         if not 3'Compatible(contig, other_contig) then
44:           if not Move3'Piece(contig, contig.next) then
45:             failure ← true
46:           else
47:             contig.next.5'adjusted ← true
48:           end if
49:         last
50:       end if
51:     end for
52:   end while
53:   compatible ← false
54:   while not failure and not compatible do
55:     for all other_contig ∈ contig_list and contig ≠ other_contig do
56:       if not 5'Compatible(contig, other_contig) then
57:         if contig.5'adjusted or not Move5'Piece(contig, contig.previous) then
58:           failure ← true
59:         end if

```

```

60:         last
61:     end if
62: end for
63: end while
64: end for
65: if length contig_list > 1
66:     hierarchical ← true
67: else
68:     hierarchical ← false
69: end if

```

where Compatible() returns true if the passed assembly piece is compatible with all of the pieces in the passed contig; otherwise returns false;

where 3'Compatible() returns true if the 3' terminus of the first passed contig is compatible with the second passed contig; otherwise returns false;

where 5'Compatible() returns true if the 5' terminus of the first passed contig is compatible with the second passed contig; otherwise returns false;

where Move3'Piece() returns true if the 3' assembly piece of the first passed contig is compatible with each piece contained within the second passed contig. If so, moves the 3' assembly piece of the first passed contig to the 5' end of the second passed contig; otherwise returns false;

where Move5'Piece() returns true if the 5' assembly piece of the first passed contig is compatible with each piece contained within the second passed contig. If so, moves the 5' assembly piece of the first passed contig to the 3' end of the second passed contig; otherwise returns false;

If a hierarchical assembly strategy cannot be found to mitigate the identified assembly piece incompatibilities, it is likely that a manual user adjustment (such as breaking a part into two sub-parts) will be required to design a successful assembly. For example, consider a variation of the assembly task shown in Figure S2A in which fragments "3" and "4" are a single contiguous assembly piece. The 5' end of this contiguous piece would be incompatible with the immediately downstream fragment "5", and the 3' end would be incompatible with the immediately upstream fragment "2". These incompatibilities are not able to be resolved using a hierarchical assembly strategy. However, as shown in Figure S2A, splitting this contiguous assembly piece into separate fragments "3" and "4", it is possible to identify a workable hierarchical assembly strategy. Further development will target the identification of such assembly piece splitting resolutions to incompatibilities that cannot be hierarchically resolved. It should be pointed out that Algorithm S3 is also directly applicable to the in vivo yeast method DNA assembler (13), which also uses sequence homology to direct the assembly process.

While the case for a hierarchical assembly mitigation strategy is clear for the example shown in Figure S2A with two sequence-identical assembly junctions ("1" to "2", and "5" to "6"), the inverse relationship between assembly junction similarity and assembly efficiency has yet to be quantitatively explored. A reasonable way to approach this would be to capture the assembly efficiency (i.e., success rate) of each reaction as an integral part of the workflow depicted in Figure S9. This large accumulated meta-data set could then be continually analyzed towards a refined quantitative relationship between assembly efficiency and junction similarity, which would inform the cost-benefit calculus for one-pot vs. hierarchical assembly strategies.

Algorithm S4: Search for the optimal set of Golden Gate assembly piece overhangs

The Golden Gate assembly method (6) utilizes 4-bp 5' overhang sequences to direct the assembly process. If two or more overhang sequences are sufficiently cohesive to a cognate overhang (e.g. the blue and grey bottom overhangs are both cohesive to the blue top overhang shown in Figure S2D), there is an ambiguity in the assembly process, which can lead to undesirable products (e.g. pieces assembled in the incorrect order or sections missing altogether). These overhang sequences are thus said to be incompatible with one another. Algorithm S4 first identifies putative overhang sequence regions (constrained by the maximum oligo size and the extents of combinatorial sequence identity about each assembly junction) and then searches these regions

for the set of overhang sequences that are compatible with themselves and each other, and that are as neutral as possible (see Figure S2E). If no set of compatible Golden Gate overhangs is found, an error message is issued.

```
1: for all junction ∈ junction_list do
2:   GenerateOverhangList(junction)
4:   sort junction.full_overhang_list by increasing Position()
5:   for all overhang ∈ junction.full_overhang_list do
6:     if not Compatible(overhang)
7:       Remove(overhang)
8:     else
9:       for all prior_overhang ∈ junction.full_overhang_list before overhang do
10:        if prior_overhang = overhang
11:          Remove(overhang)
12:        last
13:        end if
14:      end for
15:    end if
16:  end for
17: end for
18: undefine stable
19: current_junction ← First(junction_list)
20: current_junction.overhang_list ← junction.full_overhang_list
21: resume ← false
22: while true do
23:   if not FindCompatibleOverhangs(junction_list, stable, current_junction, resume)
24:     last
25:   end if
26:   resume ← true
27:   if not defined best or MaxPosition(junction_list) < max
28:     best ← junction_list
29:     max ← MaxPosition(junction_list)
30:     for all junction ∈ junction_list do
31:       for all overhang ∈ junction.full_overhang_list do
32:         if Position(overhang) > max then
33:           Remove(overhang)
34:         end if
35:       end for
36:       for all prior ∈ junction_list before junction do
37:         for all overhang ∈ junction.prior.full_overhang_list do
38:           if Position(overhang) > max then
39:             Remove(overhang)
40:           end if
41:         end for
42:       end for
43:     end for
44:   end if
45: end while

46: procedure FindCompatibleOverhangs(junction_list, stable, junction, resume)
47:   while true do
48:     for all prior ∈ junction_list after stable before junction do
49:       if prior = First(junction_list) then
```

```

50:         junction.prior.overhang_list ← junction.full_overhang_list
51:     else
52:         junction.prior.overhang_list ← junction.Previous(prior).overhang_list
53:     end if
54:     for all overhang ∈ junction.prior.overhang_list do
55:         if not Compatible(prior.current_overhang, overhang)
56:             Remove(overhang)
57:         end if
58:     end for
59:     if junction = Last(junction_list) and resume
60:         Remove(First(junction.Previous(junction).overhang_list))
61:     end if
62:     if junction = First(junction_list) then
63:         junction.current_overhang ← First(junction.overhang_list)
64:     else
65:         junction.current_overhang ← First(Previous(junction).overhang_list)
66:     end if
67:     while not defined junction.current_overhang do
68:         if junction = First(junction_list) then
69:             return false
70:         end if
71:         junction ← Previous(junction)
72:         stable ← Previous(junction)
73:         repeat
74:             if junction = First(junction_list) then
75:                 Remove(junction.current_overhang)
76:                 junction.current_overhang ← First(junction.overhang_list)
77:             else
78:                 Remove(junction.Previous(junction).current_overhang)
79:                 junction.current_overhang ← First(junction.Previous(junction).overhang_list)
80:             end if
81:             until not (defined junction.current_overhang and RedundantSearchPath(junction))
82:         end while
83:     if junction = Last(junction_list) then
84:         return true
85:     else
86:         junction ← Next(junction)
87:     end while
88: end procedure

```

```

89: procedure RedundantSearchPath(junction_list, junction)
90:     for all prior ∈ junction_list before junction do
91:         if junction.current_overhang ∈ prior.overhang_list and
92:             prior.current_overhang ∈ junction.overhang_list then
93:                 if Max(Position(junction.current_overhang), Position(prior.current_overhang)) >
94:                     Max(Position(junction.overhang_list.(prior.current_overhang)),
95:                         Position(prior.overhang_list.(junction.current_overhang))) then
96:                     return true
97:                 else if Max(Position(junction.current_overhang), Position(prior.current_overhang)) =
98:                     Max(Position(junction.overhang_list.(prior.current_overhang)),
99:                         Position(prior.overhang_list.(junction.current_overhang))) then
101:                 if junction.current_overhang ∈ junction.overhang_list after
102:                     prior.current_overhang ∈ junction.overhang_list then
103:                     return true

```

```

104:         end if
105:     end if
106: end if
107: end for
108: return false
109: end procedure

```

where `GenerateOverhangList()` returns the list of putative 4-bp overhangs that are located within the putative overhang sequence region (see Figure S2E) that spans the assembly junction (constrained by the maximum oligo size and the extents of combinatorial sequence identity about the assembly junction) from which to select a 4-bp overhang;

where `Compatible()` returns true for a single passed overhang if the overhang is compatible with itself (the maximum number of ungapped aligned identities (all frame shifts, both strands) is below threshold, see Figure S2D); similarly returns true for two passed overhangs if the two overhang sequences are compatible with one another (see Figure S2D); utilizes a hash lookup table to avoid redundant calculations; otherwise returns false;

where `Position()` returns the relative overhang position in bp from neutral (see Figure S2E);

where `MaxPosition()` returns the maximum relative overhang position in bp from neutral across all assembly junctions;

If no set of compatible set of Golden Gate overhangs is found, it is likely that a manual user adjustment (such as adding scar sequences at one or more assembly piece junctions) will be required to design a successful assembly. Further development will target the automated design of minimal scar sequences that allow for a compatible set of Golden Gate overhangs to be identified. A scar-less alternative option is to utilize a variant of Algorithm S3 to design a hierarchical Golden Gate assembly, analogous to that shown in Figure S2A-C. Further development will target the automated design of this alternative hierarchical Golden Gate assembly strategy. It should be pointed out that Algorithm S4 is also directly applicable to the USER DNA assembly methodology (14), which also uses overhang sequences (although frequently longer than 4-bp) to direct the assembly process. A variant of Algorithm S4 could also be applied to (combinatorial) SLIC, Gibson, CPEC, *in vivo* yeast DNA assembler, or other methods, and would likely be preferable to the utilization of hierarchical assembly processes (depicted in Figure S2A-C and designed by Algorithm S3) wherever possible. Further development will target the application of Algorithm S4 to designing these homology sequence recombination methodologies.

Algorithm S4 utilizes dynamic programming to reduce search complexity. Algorithm S4 stores previous compatible/incompatible overhang sequence calculations in a look-up table (the `Compatible()` procedure), recursively determines the residual set of overhang sequences to choose from at each junction (see for example pseudo-code line 52), and dynamically avoids redundant search paths (the `RedundantSearchPath()` procedure). For many simple Golden Gate assembly designs, the complexity of Algorithm S4 may appear to be overkill. However, we have found that as the number of assembly pieces approaches (or narrowly exceeds) ten, and/or if the sequences spanning assembly junctions are highly homologous (e.g. repeated or highly similar RBS sites), the search process needs to be kept as efficient as possible to terminate in a reasonable amount of time. This is because the complexity of the exhaustive search for compatible Golden Gate overhang sequences is roughly $O(M^N)$, where M is the number of overhang sequences to choose from for each junction, and N is the number of junctions. Algorithm S4 is not embarrassingly parallelizable since the optimal search process is dependent on the characteristics of the best compatible overhang set found so far. Nevertheless, it would be possible to parallelize it (without inducing too much waste) by tasking each thread/process with a subset of the overhang possibilities for the first junction(s) and having each thread/process broadcast their best set parameters as they are found. As the price of direct DNA synthesis continues to fall, and replaces the need for embedding sequence resulting from non-neutral overhang position selection into the corresponding primers, there will be less of a premium placed on maximizing the neutrality of the overhang positions, and more of an emphasis on compatibility stringency. This change in emphasis will not require any change to Algorithm S4, but will rather just require a perturbation to the stringency of the `Compatible()` function and an extension of the putative overhang sequence regions beyond what is currently constrained by the maximum oligo length.

Algorithm S5: Closely approximate the optimal distribution of PCR reactions in multi-well plates across thermocycler block annealing temperature zone gradient(s)

Depending on the design of a given DNA assembly process, PCR may be required to generate (some of) the assembly pieces. While primer and flanking homology sequence design attempt to constrain melting temperature to a narrow acceptable range where possible (see Algorithm S2), extreme %GC template composition may skew the resulting temperatures to well below (AT-rich) or above (GC-rich) the targeted optimum. Most modern thermocyclers feature standardized multi-well format blocks, and some (such as the Applied Biosystems Veriti Thermal Cycler employed in this study) now feature temperature gradients with individually controllable annealing temperature zones. Algorithm S5 takes as input a set of PCR reactions with target annealing temperatures, taken here to be the minimum of the forward and reverse primer melting temperatures + 2 °C, and optimizes the annealing temperature zones of the thermocycler block(s) and the distribution of the PCR reactions (in multi-well plates) across the zones so as to minimize the objective function, namely the summed difference squared between the targeted annealing temperatures of the PCR reactions and the actual annealing temperatures of the thermocycler zones in which they are placed (as shown in Figure S5E). Algorithm S5 exploits a Monte-Carlo simulated annealing approach to converge upon the optimal distribution. Simulated annealing is a classical computational technique to find global minima in discrete search spaces with complicated energy landscapes. This approach is well suited to the optimization problem addressed by Algorithm S5 because the search space (the placement of each PCR reaction in its own well, and the annealing temperature of each zone) is discrete, and there is a complicated relationship between zone temperatures, PCR reaction placements, and the objective function to be minimized.

```
1: number_blocks = MinBlocksRequired(reaction_list) - 1
2: repeat
3:   number_blocks ← number_blocks + 1
4:   block_list ← InitializeBlocks(number_blocks, reaction_list)
5:   FillBlocks(block_list, reaction_list)
6:   current ← Objective(block_list, reaction_list)
7:   best ← current
8:   current_temperature ← initial
9:   for all move ← 1, n do
10:    trial_list ← block_list
11:    TrialMove(trial_list)
12:    FillBlocks(trial_list, reaction_list)
13:    trial ← Objective(trial_list, reaction_list)
14:    if trial < current or Random() < Exp((current - trial)/current_temperature) then
15:      block_list ← trial_list
16:      current ← trial
17:      if current ≤ best then
18:        best ← current
19:        best_block_list ← block_list
20:      end if
21:    end if
22:    current_temperature ← current_temperature - (initial - final)/n
23:  end for
24: until MaxDeviance(best_block_list, reaction_list) < threshold
```

where MinBlocksRequired() returns the minimum number of thermocycler blocks required to contain all of the PCR reactions;

where InitializeBlocks() returns a set of the specified number of thermocycler blocks whose zone annealing temperatures have been initialized to span from the lowest optimal annealing temperature across the PCR reactions to the highest optimal annealing temperature across the PCR reactions (or highest temperature that can be achieved given temperature gradient limitations) with linear step annealing temperature increases between zones;

where FillBlocks() fills the thermocycler blocks with the PCR reactions; repeats the following procedure for each PCR reaction sorted from lowest to highest optimal annealing temperature: given the zone annealing temperatures, identify the best zone with an empty well remaining to which to add the current PCR reaction, and deposit the PCR reaction in this zone; after depositing all of the PCR reactions into the thermocycler block(s), rearrange the PCR reactions in place (same thermocycler wells) such that the annealing temperatures of the PCR reactions are sorted monotonically from low to high with the increasing zone annealing temperature gradient;

where Objective() returns the sum of the difference squared between the optimal annealing temperature of each PCR reaction and the actual annealing temperature of the zone it has been placed in;

where TrialMove() randomly select one of the zones within the specified thermocycler blocks, and randomly perturbs the annealing temperature of the zone by either adding or subtracting a delta temperature; if this perturbation collaterally affects adjacent zones (due to temperature gradient limitations) adjust the temperatures of the affected zones accordingly;

where Random() returns a number from the half-closed interval [0,1) with uniform probability;

where MaxDeviance() returns the maximum temperature deviance between the optimal annealing temperature of a PCR reaction and the actual annealing temperature of the zone it has been placed in.

Depending on the parameters selected and search scheme adopted, simulated annealing can act as a random search, prematurely converge on local minima, or converge on the desired global minimum. It is crucial to explore the search space sufficiently well so as to ensure confidence that the global minimum has been encountered, but an excessive number of trial moves is computationally wasteful. Some of the parameters (e.g., MAXDELTA TEMPERATURE ADJACENT ZONES, NCOLUMNS MULTIWELLPLATE, NROWS MULTIWELLPLATE, WELLS PER THERMOCYCLER ZONE, ZONES PER THERMOCYCLER BLOCK, and TRIAL DELTA TEMPERATURE) governing Algorithm S5 are determined by thermocycler specifications and multi-well plate format geometry. The MAX DELTA TEMPERATURE REACTION OPTIMUM ZONE ACCEPTABLE parameter is determined by the experimental preference of the user. Two parameters in particular (MAX MC STEPS PER ZONE and MC TEMPERATURE INITIAL) determine whether Algorithm S5 acts as a random search, or converges on local or global minima. Figure S6 shows Algorithm S5 convergence as a function of MAX MC STEPS PER ZONE and MC TEMPERATURE INITIAL. The default parameters for j5 (MC TEMPERATURE INITIAL = 0.1 and MAX MC STEPS PER ZONE = 1000) are set conservatively so as remain putatively effective for more frustrated searches than that pursued in Figure S6.

For simple DNA assembly designs that do not require too many PCR reactions, Algorithm S5 may seem excessive. In addition, anecdotal experience may suggest that precisely tuning the annealing temperature for a given PCR reaction might not yield significantly superior PCR results, since the optimal annealing temperature range may be fairly broad (spanning several °C) for any given PCR reaction. While these points are well taken, it should be pointed out that multiple small assembly tasks can be condensed into a sizable meta-assembly project (see Results) with many collective prerequisite PCR reactions, and furthermore, there is no compelling reason not to exploit available thermocycler gradient features if the design process is automated and effectively effortless. Sets of PCR reactions with non-uniformly distributed target annealing temperatures with extreme highs and lows will be the most likely to derive benefit from Algorithm S5.

Algorithm S5 would need to be adjusted for a strictly linear (non-zone type) gradient thermocycler (such as a MJ Research Tetrad PTC-225 Thermo Cycler). This could be accomplished by modifying the subroutine that generates the initial distribution of zone temperatures, and changing the Monte Carlo move set such that either of the linear gradient temperature extremes may be perturbed, and internal intermediate zones are linearly adjusted accordingly. Further development will focus on an implementation variant of Algorithm S5 for strictly linear thermocycler gradient blocks.

REFERENCES

1. Khlebnikov, A., Datsenko, K. A., Skaug, T., Wanner, B. L., and Keasling, J. D. (2001) Homogeneous expression of the P(BAD) promoter in *Escherichia coli* by constitutive expression of the low-affinity high-capacity AraE transporter, *Microbiology* 147, 3241-3247.
2. Gibson, D. G., Young, L., Chuang, R. Y., Venter, J. C., Hutchison, C. A., 3rd, and Smith, H. O. (2009) Enzymatic assembly of DNA molecules up to several hundred kilobases, *Nat Methods* 6, 343-345.
3. Li, M. Z., and Elledge, S. J. (2007) Harnessing homologous recombination in vitro to generate recombinant DNA via SLIC, *Nat Methods* 4, 251-256.
4. Quan, J., and Tian, J. (2009) Circular polymerase extension cloning of complex gene libraries and pathways, *PLoS One* 4, e6441.
5. Engler, C., Gruetzner, R., Kandzia, R., and Marillonnet, S. (2009) Golden gate shuffling: a one-pot DNA shuffling method based on type IIs restriction enzymes, *PLoS One* 4, e5553.
6. Engler, C., Kandzia, R., and Marillonnet, S. (2008) A one pot, one step, precision cloning method with high throughput capability, *PLoS One* 3, e3647.
7. Yu, B. J., Kang, K. H., Lee, J. H., Sung, B. H., Kim, M. S., and Kim, S. C. (2008) Rapid and efficient construction of markerless deletions in the *Escherichia coli* genome, *Nucleic Acids Res* 36, e84.
8. Musso, M., Bocciardi, R., Parodi, S., Ravazzolo, R., and Ceccherini, I. (2006) Betaine, dimethyl sulfoxide, and 7-deaza-dGTP, a powerful mixture for amplification of GC-rich DNA sequences, *J Mol Diagn* 8, 544-550.
9. Bilitchenko, L., Liu, A., Cheung, S., Weeding, E., Xia, B., Leguia, M., Anderson, J. C., and Densmore, D. (2011) Eugene--a domain specific language for specifying and constraining synthetic biological parts, devices, and systems, *PLoS One* 6, e18882.
10. Bilitchenko, L., Liu, A., and Densmore, D. (2011) The Eugene language for synthetic biology, *Methods Enzymol* 498, 153-172.
11. Rozen, S., and Skaletsky, H. (2000) Primer3 on the WWW for general users and for biologist programmers, *Methods Mol Biol* 132, 365-386.
12. Zhang, Z., Schwartz, S., Wagner, L., and Miller, W. (2000) A greedy algorithm for aligning DNA sequences, *J Comput Biol* 7, 203-214.
13. Shao, Z., and Zhao, H. (2009) DNA assembler, an in vivo genetic method for rapid construction of biochemical pathways, *Nucleic Acids Res* 37, e16.
14. Bitinaite, J., Rubino, M., Varma, K. H., Schildkraut, I., Vaisvila, R., and Vaiskunaite, R. (2007) USER friendly DNA engineering and cloning method by uracil excision, *Nucleic Acids Res* 35, 1992-2002.